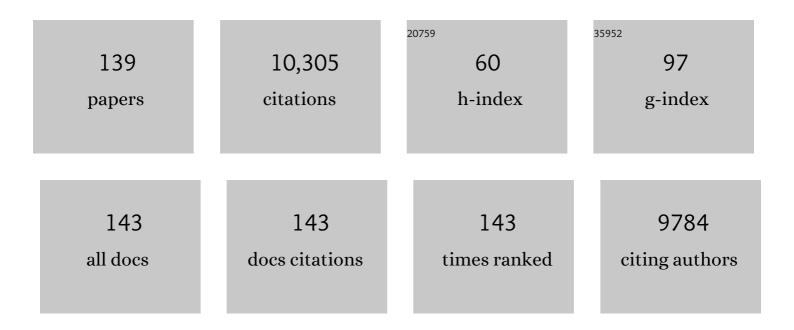
List of Publications by Year in descending order

Source: https://exaly.com/author-pdf/1343737/publications.pdf Version: 2024-02-01



#	Article	IF	CITATIONS
1	An ultra-sensitive and rapid response speed graphene pressure sensors for electronic skin and health monitoring. Nano Energy, 2016, 23, 7-14.	8.2	467
2	New insights and perspectives into biological materials for flexible electronics. Chemical Society Reviews, 2017, 46, 6764-6815.	18.7	322
3	Highâ€performance flexible sensing devices based on polyaniline/MXene nanocomposites. InformaÄnÃ- Materišly, 2019, 1, 407-416.	8.5	310
4	Bioinspired Interlocked Structure-Induced High Deformability for Two-Dimensional Titanium Carbide (MXene)/Natural Microcapsule-Based Flexible Pressure Sensors. ACS Nano, 2019, 13, 9139-9147.	7.3	308
5	Vitrimer Elastomerâ€Based Jigsaw Puzzleâ€Like Healable Triboelectric Nanogenerator for Selfâ€Powered Wearable Electronics. Advanced Materials, 2018, 30, e1705918.	11.1	265
6	Encapsuled nanoreactors (Au@SnO2): a new sensing material for chemical sensors. Nanoscale, 2013, 5, 2686.	2.8	243
7	Branch-like Hierarchical Heterostructure (α-Fe <sub>2</sub> O <sub>3</sub> /TiO <sub>2</sub> ): A Novel Sensing Material for Trimethylamine Gas Sensor. ACS Applied Materials & Interfaces, 2013, 5, 12310-12316.	4.0	230
8	Recent Progress of Selfâ€Powered Sensing Systems for Wearable Electronics. Small, 2017, 13, 1701791.	5.2	223
9	Metal–Organic Frameworks-Derived Hierarchical Co <sub>3</sub> O <sub>4</sub> Structures as Efficient Sensing Materials for Acetone Detection. ACS Applied Materials & Interfaces, 2018, 10, 9765-9773.	4.0	215
10	Reviews of wearable healthcare systems: Materials, devices and system integration. Materials Science and Engineering Reports, 2020, 140, 100523.	14.8	215
11	Three-Dimensional Hierarchical Flowerlike α-Fe <sub>2</sub> O <sub>3</sub> Nanostructures: Synthesis and Ethanol-Sensing Properties. ACS Applied Materials & Interfaces, 2011, 3, 4689-4694.	4.0	214
12	Carbon-Reinforced Nb <sub>2</sub> CT <sub>x</sub> MXene/MoS <sub>2</sub> Nanosheets as a Superior Rate and High-Capacity Anode for Sodium-Ion Batteries. ACS Nano, 2021, 15, 7439-7450.	7.3	203
13	Ultrasensitive and ultraflexible e-skins with dual functionalities for wearable electronics. Nano Energy, 2017, 38, 28-35.	8.2	194
14	P-type Co3O4 nanomaterials-based gas sensor: Preparation and acetone sensing performance. Sensors and Actuators B: Chemical, 2017, 242, 369-377.	4.0	184
15	Ethanol Gas Detection Using a Yolk-Shell (Core-Shell) α-Fe <sub>2</sub> O <sub>3</sub> Nanospheres as Sensing Material. ACS Applied Materials & Interfaces, 2015, 7, 13098-13104.	4.0	170
16	High-performance, flexible electronic skin sensor incorporating natural microcapsule actuators. Nano Energy, 2017, 36, 38-45.	8.2	160
17	Microbe-Assisted Assembly of Ti <sub>3</sub> C <sub>2</sub> T <sub><i>x</i></sub> MXene on Fungi-Derived Nanoribbon Heterostructures for Ultrastable Sodium and Potassium Ion Storage. ACS Nano, 2021, 15, 3423-3433.	7.3	158
18	Biomimetic, biocompatible and robust silk Fibroin-MXene film with stable 3D cross-link structure for flexible pressure sensors. Nano Energy, 2020, 78, 105252.	8.2	153

#	Article	IF	CITATIONS
19	Controlled Assembly of MXene Nanosheets as an Electrode and Active Layer for Highâ€Performance Electronic Skin. Advanced Functional Materials, 2021, 31, 2010533.	7.8	143
20	Cross-linked p-type Co3O4 octahedral nanoparticles in 1D n-type TiO2 nanofibers for high-performance sensing devices. Journal of Materials Chemistry A, 2014, 2, 10022.	5.2	135
21	Hybrid Co <sub>3</sub> O <sub>4</sub> /SnO <sub>2</sub> Core–Shell Nanospheres as Real-Time Rapid-Response Sensors for Ammonia Gas. ACS Applied Materials & Interfaces, 2016, 8, 6539-6545.	4.0	134
22	Recent Advances in Smart Wearable Sensing Systems. Advanced Materials Technologies, 2018, 3, 1800444.	3.0	128
23	Ti <sub>3</sub> C <sub>2</sub> T <i><sub>x</sub></i> MXene Conductive Layers Supported Bioâ€Derived Fe <i><sub>x</sub></i> <sub>a^'1</sub> Se <i><sub>x</sub></i> /MXene/Carbonaceous Nanoribbons for Highâ€Performance Half/Full Sodiumâ€Ion and Potassiumâ€Ion Batteries. Advanced Materials, 2021, 33, e2101535.	11.1	128
24	Flexible Selfâ€Powered Integrated Sensing System with 3D Periodic Ordered Black Phosphorus@MXene Thinâ€Films. Advanced Materials, 2021, 33, e2007890.	11.1	127
25	Flexible, Grapheneâ€Coated Biocomposite for Highly Sensitive, Realâ€Time Molecular Detection. Advanced Functional Materials, 2016, 26, 8623-8630.	7.8	116
26	Templating synthesis of ZnO hollow nanospheres loaded with Au nanoparticles and their enhanced gas sensing properties. Journal of Materials Chemistry, 2012, 22, 4767.	6.7	115
27	Bioâ€Multifunctional Smart Wearable Sensors for Medical Devices. Advanced Intelligent Systems, 2019, 1, 1900040.	3.3	115
28	Hollow ZnSnO <sub>3</sub> Cubes with Controllable Shells Enabling Highly Efficient Chemical Sensing Detection of Formaldehyde Vapors. ACS Applied Materials & Interfaces, 2017, 9, 14525-14533.	4.0	110
29	Grainâ€Boundaryâ€Induced Drastic Sensing Performance Enhancement of Polycrystallineâ€Microwire Printed Gas Sensors. Advanced Materials, 2019, 31, e1804583.	11.1	110
30	Enhanced sensing performance of the Co3O4 hierarchical nanorods to NH3 gas. Sensors and Actuators B: Chemical, 2015, 209, 449-455.	4.0	104
31	Highly-stable polymer-crosslinked 2D MXene-based flexible biocompatible electronic skins for in vivo biomonitoring. Nano Energy, 2021, 84, 105921.	8.2	104
32	Zinc oxide core–shell hollow microspheres with multi-shelled architecture for gas sensor applications. Journal of Materials Chemistry, 2011, 21, 19331.	6.7	100
33	Plantâ€Based Modular Building Blocks for "Green―Electronic Skins. Advanced Functional Materials, 2018, 28, 1804510.	7.8	97
34	Design of CuO–TiO <sub>2</sub> heterostructure nanofibers and their sensing performance. Journal of Materials Chemistry A, 2014, 2, 9030-9034.	5.2	94
35	Enhanced ammonia sensing performances of Pd-sensitized flowerlike ZnO nanostructure. Sensors and Actuators B: Chemical, 2011, 156, 395-400.	4.0	92
36	Facile synthesis and enhanced ethanol sensing properties of the brush-like ZnO–TiO2 heterojunctions nanofibers. Sensors and Actuators B: Chemical, 2013, 184, 21-26.	4.0	92

#	Article	IF	CITATIONS
37	Artificial Optoelectronic Synapses Based on TiN <i><sub>x</sub></i> O <sub>2–</sub> <i><sub>x</sub></i> /MoS <sub>2</sub> Heterojunction for Neuromorphic Computing and Visual System. Advanced Functional Materials, 2021, 31, 2101201.	7.8	92
38	3D Chemical Cross‣inking Structure of Black Phosphorus@CNTs Hybrid as a Promising Anode Material for Lithium Ion Batteries. Advanced Functional Materials, 2020, 30, 1909372.	7.8	92
39	Nanoparticles-assembled Co3O4 nanorods p-type nanomaterials: One-pot synthesis and toluene-sensing properties. Sensors and Actuators B: Chemical, 2014, 201, 1-6.	4.0	90
40	Enhanced acetone sensing performances of hierarchical hollow Au-loaded NiO hybrid structures. Sensors and Actuators B: Chemical, 2012, 161, 178-183.	4.0	84
41	P-type octahedral Cu 2 O particles with exposed {111} facets and superior CO sensing properties. Sensors and Actuators B: Chemical, 2017, 239, 211-217.	4.0	83
42	Microâ€Nano Processing of Active Layers in Flexible Tactile Sensors via Template Methods: A Review. Small, 2021, 17, e2100804.	5.2	82
43	Wearable, Implantable, and Interventional Medical Devices Based on Smart Electronic Skins. Advanced Materials Technologies, 2021, 6, 2100107.	3.0	81
44	Sweatâ€Permeable, Biodegradable, Transparent and Selfâ€powered Chitosanâ€Based Electronic Skin with Ultrathin Elastic Gold Nanofibers. Advanced Functional Materials, 2022, 32, .	7.8	80
45	A flexible, ultra-sensitive chemical sensor with 3D biomimetic templating for diabetes-related acetone detection. Journal of Materials Chemistry B, 2017, 5, 4019-4024.	2.9	76
46	Orthorhombic KSc2F7:Yb/Er nanorods: controlled synthesis and strong red upconversion emission. Nanoscale, 2013, 5, 11928.	2.8	75
47	Grapheneâ€Functionalized Natural Microcapsules: Modular Building Blocks for Ultrahigh Sensitivity Bioelectronic Platforms. Advanced Functional Materials, 2016, 26, 2097-2103.	7.8	75
48	Nearâ€Infrared Light Triggered Selfâ€Powered Mechanoâ€Optical Communication System using Wearable Photodetector Textile. Advanced Functional Materials, 2021, 31, 2104782.	7.8	74
49	Enhanced Photoluminescence of Water Soluble YVO <sub>4</sub> :Ln <sup>3+</sup> (Ln = Eu, Dy, Sm,) Tj ETQq1 17042-17045.	1 0.7843 1.5	14 rgBT /O 73
50	Template-free synthesized hollow NiO–SnO2 nanospheres with high gas-sensing performance. Sensors and Actuators B: Chemical, 2012, 164, 90-95.	4.0	73
51	Toluene and ethanol sensing performances of pristine and PdO-decorated flower-like ZnO structures. Sensors and Actuators B: Chemical, 2013, 176, 323-329.	4.0	73
52	Enhanced deep-ultraviolet upconversion emission of Gd3+ sensitized by Yb3+ and Ho3+ in β-NaLuF4 microcrystals under 980 nm excitation. Journal of Materials Chemistry C, 2013, 1, 2485.	2.7	72
53	Concave Cu 2 O octahedral nanoparticles as an advanced sensing material for benzene (C 6 H 6 ) and nitrogen dioxide (NO 2 ) detection. Sensors and Actuators B: Chemical, 2016, 223, 311-317.	4.0	72
54	Self-assembled CdS quantum dots in carbon nanotubes: induced polysulfide trapping and redox kinetics enhancement for improved lithium–sulfur battery performance. Journal of Materials Chemistry A, 2019, 7, 806-815.	5.2	72

#	Article	IF	CITATIONS
55	Assembling Co3O4 Nanoparticles into MXene with Enhanced electrochemical performance for advanced asymmetric supercapacitors. Journal of Colloid and Interface Science, 2021, 599, 109-118.	5.0	72
56	Wearable Sweat Loss Measuring Devices: From the Role of Sweat Loss to Advanced Mechanisms and Designs. Advanced Science, 2022, 9, e2103257.	5.6	69
57	Structure-driven efficient NiFe2O4 materials for ultra-fast response electronic sensing platform. Sensors and Actuators B: Chemical, 2018, 255, 1436-1444.	4.0	65
58	Assessment of Occlusal Force and Local Gas Release Using Degradable Bacterial Cellulose/Ti <sub>3</sub> C <sub>2</sub> T <sub><i>x</i></sub> MXene Bioaerogel for Oral Healthcare. ACS Nano, 2021, 15, 18385-18393.	7.3	65
59	Nanofiber/nanowires-based flexible and stretchable sensors. Journal of Semiconductors, 2020, 41, 041605.	2.0	64
60	Fabrication of flower-like ZnO nanosheet and nanorod-assembled hierarchical structures and their enhanced performance in gas sensors. New Journal of Chemistry, 2014, 38, 84-89.	1.4	62
61	Comparison of toluene sensing performances of zinc stannate with different morphology-based gas sensors. Sensors and Actuators B: Chemical, 2016, 227, 448-455.	4.0	62
62	Highly sensitive sensing platform based on ZnSnO 3 hollow cubes for detection of ethanol. Applied Surface Science, 2017, 400, 262-268.	3.1	60
63	Programmable three-dimensional advanced materials based on nanostructures as building blocks for flexible sensors. Nano Today, 2019, 26, 176-198.	6.2	60
64	Metal Sulfides@Carbon Microfiber Networks for Boosting Lithium Ion/Sodium Ion Storage via a General Metal– <i>Aspergillus niger</i> Bioleaching Strategy. ACS Applied Materials & Interfaces, 2019, 11, 8072-8080.	4.0	58
65	Controlled synthesis and luminescence properties from cubic to hexagonal NaYF4:Ln3+ (Ln=Eu and) Tj ETQq1 1	0.784314 2.8	rgBT /Overic
66	Synthesis and ethanol sensing properties of SnO2 nanosheets via a simple hydrothermal route. Solid-State Electronics, 2012, 76, 91-94.	0.8	57
67	Highly Stable Crossâ€Linked Cationic Polyacrylamide/Ti <sub>3</sub> C <sub>2</sub> T <sub>x</sub> MXene Nanocomposites for Flexible Ammoniaâ€Recognition Devices. Advanced Materials Technologies, 2020, 5, 2000248.	3.0	56
68	An Integrated Flexible Allâ€Nanowire Infrared Sensing System with Record Photosensitivity. Advanced Materials, 2020, 32, e1908419.	11.1	56
69	Hierarchical structure with heterogeneous phase as high performance sensing materials for trimethylamine gas detecting. Sensors and Actuators B: Chemical, 2015, 220, 1224-1231.	4.0	55
70	Ring-like PdO-decorated NiO with lamellar structures and their application in gas sensor. Sensors and Actuators B: Chemical, 2012, 171-172, 1180-1185.	4.0	54
71	Controllable and enhanced HCHO sensing performances of different-shelled ZnO hollow microspheres. Sensors and Actuators B: Chemical, 2013, 183, 467-473.	4.0	53
72	Self-assembled Cobalt-doped NiMn-layered double hydroxide (LDH)/V2CT MXene hybrids for advanced aqueous electrochemical energy storage properties. Chemical Engineering Journal, 2022, 430, 132992.	6.6	53

#	Article	IF	CITATIONS
73	Synthesis of rattle-type SnO2 structures with porous shells. Journal of Materials Chemistry, 2012, 22, 18111.	6.7	51
74	MXene quantum dot within natural 3D watermelon peel matrix for biocompatible flexible sensing platform. Nano Research, 2022, 15, 3653-3659.	5.8	51
75	A class of hierarchical nanostructures: ZnO surface-functionalized TiO2 with enhanced sensing properties. RSC Advances, 2013, 3, 3131.	1.7	49
76	MXene-Bonded hollow MoS2/Carbon sphere strategy for high-performance flexible sodium ion storage. Chemical Engineering Journal, 2022, 430, 132755.	6.6	49
77	Ring-like PdO–NiO with lamellar structure for gas sensor application. Journal of Materials Chemistry, 2012, 22, 12453.	6.7	48
78	Facile synthesis of hierarchical SnO2 semiconductor microspheres for gas sensor application. Sensors and Actuators B: Chemical, 2011, 155, 285-289.	4.0	46
79	Biocompatible and Biodegradable Functional Polysaccharides for Flexible Humidity Sensors. Research, 2020, 2020, 8716847.	2.8	46
80	Highly sensitive hybrid nanofiber-based room-temperature CO sensors: Experiments and density functional theory simulations. Nano Research, 2018, 11, 1029-1037.	5.8	44
81	TiVCT <i><sub>x</sub></i> MXene/Chalcogenide Heterostructureâ€Based Highâ€Performance Magnesiumâ€ion Battery as Flexible Integrated Units. Small, 2022, 18, .	5.2	44
82	High-selective sensitive NH 3 gas sensor: A density functional theory study. Sensors and Actuators B: Chemical, 2018, 263, 502-507.	4.0	43
83	Constructing Hierarchical Heterostructured Mn <sub>3</sub> O <sub>4</sub> /Zn <sub>2</sub> SnO <sub>4</sub> Materials for Efficient Gas Sensing Reaction. Advanced Materials Interfaces, 2018, 5, 1800115.	1.9	42
84	Ultraviolet and violet upconversion fluorescence of europium (III) doped in YF_3 nanocrystals. Optics Letters, 2009, 34, 2781.	1.7	41
85	Rapid sensitive sensing platform based on yolk-shell hybrid hollow sphere for detection of ethanol. Sensors and Actuators B: Chemical, 2018, 256, 479-487.	4.0	40
86	A Flexible Humidity Sensor Based on Natural Biocompatible Silk Fibroin Films. Advanced Materials Technologies, 2021, 6, .	3.0	39
87	Reduced graphite oxide/SnO <sub>2</sub> /Au hybrid nanomaterials for NO <sub>2</sub> sensing performance at relatively low operating temperature. RSC Advances, 2014, 4, 57436-57441.	1.7	38
88	MXene/ZIF-67/PAN Nanofiber Film for Ultra-sensitive Pressure Sensors. ACS Applied Materials & Interfaces, 2022, 14, 12367-12374.	4.0	38
89	Fast and real-time acetone gas sensor using hybrid ZnFe <sub>2</sub> O <sub>4</sub> /ZnO hollow spheres. RSC Advances, 2016, 6, 66738-66744.	1.7	37
90	Biocompatible MXene/Chitosan-Based Flexible Bimodal Devices for Real-Time Pulse and Respiratory Rate Monitoring. , 2021, 3, 921-929.		36

#	Article	IF	CITATIONS
91	Terminal sliding mode control for full vehicle active suspension systems. Journal of Mechanical Science and Technology, 2018, 32, 2851-2866.	0.7	35
92	Constructing p–n heterostructures for efficient structure–driven ethanol sensing performance. Sensors and Actuators B: Chemical, 2018, 255, 745-753.	4.0	34
93	Upconversion emissions from high-energy states of Eu^3+ sensitized by Yb^3+ and Ho^3+ in β-NaYF_4 microcrystals under 980 nm excitation. Optics Express, 2011, 19, 25471.	1.7	32
94	Preparation of Au-sensitized 3D hollow SnO2 microspheres with an enhanced sensing performance. Journal of Alloys and Compounds, 2014, 586, 399-403.	2.8	32
95	Efficient luminescence enhancement of Gd_2O_3:Ln^3+ (Ln = Yb/Er, Eu) NCs by codoping Zn^2+ and Li^+ inert ions. Optical Materials Express, 2017, 7, 329.	1.6	32
96	Enhanced ethanol sensing properties of NiO-doped SnO2 polyhedra. New Journal of Chemistry, 2012, 36, 1003.	1.4	31
97	Ultravioletâ€Assisted Construction of Nitrogenâ€Rich Ag@Ti <sub>3</sub> C <sub>2</sub> T <i><sub>x</sub></i> MXene for Highly Efficient Hydrogen Evolution Electrocatalysis and Supercapacitor. Advanced Materials Interfaces, 2020, 7, 2001449.	1.9	31
98	Direct annealing of electrospun synthesized high-performance porous SnO2 hollow nanofibers for gas sensors. RSC Advances, 2013, 3, 9723.	1.7	30
99	NIR to VUV: Seven-Photon Upconversion Emissions from Gd <sup>3+</sup> Ions in Fluoride Nanocrystals. Journal of Physical Chemistry Letters, 2015, 6, 556-560.	2.1	30
100	Allâ€Flexible Artificial Reflex Arc Based on Thresholdâ€Switching Memristor. Advanced Functional Materials, 2022, 32, .	7.8	30
101	1D/2D heterostructure nanofiber flexible sensing device with efficient gas detectivity. Applied Surface Science, 2019, 479, 209-215.	3.1	28
102	Carbon materials-functionalized tin dioxide nanoparticles toward robust, high-performance nitrogen dioxide gas sensor. Journal of Colloid and Interface Science, 2018, 524, 76-83.	5.0	27
103	The synthesis and fast ethanol sensing properties of core–shell SnO <sub>2</sub> @ZnO composite nanospheres using carbon spheres as templates. New Journal of Chemistry, 2016, 40, 6796-6802.	1.4	26
104	Effect of alkali ions on the formation of rare earth fluoride by hydrothermal synthesis: structure tuning and size controlling. CrystEngComm, 2013, 15, 2897.	1.3	24
105	A perspective on flexible sensors in developing diagnostic devices. Applied Physics Letters, 2021, 119, .	1.5	23
106	Ultrahigh-sensitive sensing platform based on p-type dumbbell-like Co 3 O 4 network. Applied Surface Science, 2017, 426, 951-956.	3.1	21
107	Synthesis and luminescence properties of RE3+ (RE = Yb, Er, Tm, Eu, Tb)-doped Sc2O3 microcrystals. Journal of Alloys and Compounds, 2015, 653, 304-309.	2.8	20
108	Lightâ€Induced Surface Modification of Natural Plant Microparticles: Toward Colloidal Science and Cellular Adhesion Applications. Advanced Functional Materials, 2018, 28, 1707568.	7.8	20

#	Article	IF	CITATIONS
109	Highly Active Coâ€Based Catalyst in Nanofiber Matrix as Advanced Sensing Layer for High Selectivity of Flexible Sensing Device. Advanced Materials Technologies, 2018, 4, 1800521.	3.0	20
110	Ultraviolet upconversion emission of Pb <sup>2+</sup> ions sensitized by Yb <sup>3+</sup> -trimers in CaF <sub>2</sub> . RSC Advances, 2017, 7, 2676-2681.	1.7	17
111	Ultrafine Sb2S3@carbon-nanofibers for fast and stable sodium storage. Electrochimica Acta, 2022, 411, 140067.	2.6	16
112	Fast response/recovery performance of comb-like Co3O4 nanostructure. RSC Advances, 2014, 4, 21115.	1.7	14
113	Hierarchical MXene@ZIFâ€67 Film Based High Performance Tactile Sensor with Large Sensing Range from Motion Monitoring to Sound Wave Detection. Advanced Materials Technologies, 2022, 7, .	3.0	14
114	Biocompatible liquid metal coated stretchable electrospinning film for strain sensors monitoring system. Science China Materials, 2022, 65, 2235-2243.	3.5	14
115	Large-scale synthesis and photoluminescence properties ofÂSiC networks. Applied Physics A: Materials Science and Processing, 2009, 96, 521-527.	1.1	12
116	Impurity doping: a novel strategy for selective synthesis of YF <sub>3</sub> and NaYF <sub>4</sub> crystals. CrystEngComm, 2017, 19, 3215-3221.	1.3	12
117	Hydrophobic to superhydrophilic tuning of multifunctional sporopollenin for microcapsule and bio-composite applications. Applied Materials Today, 2020, 18, 100525.	2.3	12
118	Dynamic simulation and analysis of the elevating mechanism of a forklift based on a power bond graph. Journal of Mechanical Science and Technology, 2016, 30, 4043-4048.	0.7	9
119	High energy density supercapacitor based on N/B co-doped graphene nanoarchitectures and ionic liquid electrolyte. Ionics, 2019, 25, 4351-4360.	1.2	9
120	Tissueâ€Like Sodium Alginateâ€Coated 2D MXeneâ€Based Flexible Temperature Sensors for Fullâ€Range Temperature Monitoring. Advanced Materials Technologies, 2022, 7, .	3.0	9
121	Chemically Modified Silk Fibroin Hydrogel for Environment-stable Electronic Skin. Sensors and Actuators Reports, 2022, 4, 100089.	2.3	9
122	Bright Green Upconversion Fluorescence of Yb3+, Er3+-Codoped NaYF4 Nanocrystals. Journal of Nanoscience and Nanotechnology, 2010, 10, 1825-1828.	0.9	7
123	ACETONE SENSING PROPERTIES OF HIERARCHICAL ZnO URCHINLIKE STRUCTURES BY HYDROTHERMAL PROCESS. Biomedical Engineering - Applications, Basis and Communications, 2012, 24, 99-103.	0.3	7
124	Anchored SnS nanorods based on a carbon-enhanced Nb2CTx three-dimensional nanoflower framework achieve stable, high capacity Na-ion storage. Applied Surface Science, 2022, 597, 153598.	3.1	7
125	Preparation of Highly Monodisperse Electroactive Pollen Biocomposites. ChemNanoMat, 2016, 2, 414-418.	1.5	6
126	Gas Sensors: Grainâ€Boundaryâ€Induced Drastic Sensing Performance Enhancement of Polycrystallineâ€Microwire Printed Gas Sensors (Adv. Mater. 4/2019). Advanced Materials, 2019, 31, 1970028.	11.1	6

#	Article	IF	CITATIONS
127	The position shifting of charge transfer band in Eu3+-doped Re2O3 phosphors. Chemical Physics Letters, 2019, 731, 136611.	1.2	5
128	Printable Ta Substrate with High Stability and Enhanced Interface Adhesion for Flexible Supercapacitor Performance Improvement. Advanced Materials Technologies, 2019, 4, 1900338.	3.0	5
129	2D Nanomaterials with Hierarchical Architecture for Flexible Sensor Application. ACS Symposium Series, 2020, , 93-116.	0.5	5
130	The 1S0 → 3P1 transition position shift of Bi3+ ion doped Ln2O3 (Ln = Lu, Gd, La) phosphors. Journal of Luminescence, 2021, 234, 117971.	1.5	4
131	Double-color luminescence and magnetic characteristics in Fe <sup>3+</sup> doped NaErF <sub>4</sub> microcrystals. Optical Materials Express, 2019, 9, 3379.	1.6	4
132	The universal equation of state applied to analysis of EOS data for solid molybdenum and tungsten. Journal of Materials Science, 2009, 44, 708-714.	1.7	3
133	Oxidized Ti <sub>3</sub> C <sub>2</sub> T <sub>x</sub> film-based high-performance flexible pressure sensors. Journal Physics D: Applied Physics, 2021, 54, 384002.	1.3	3
134	Biosensors: Graphene-Functionalized Natural Microcapsules: Modular Building Blocks for Ultrahigh Sensitivity Bioelectronic Platforms (Adv. Funct. Mater. 13/2016). Advanced Functional Materials, 2016, 26, 2220-2220.	7.8	1
135	Enhanced down-conversion luminescence properties of CaSc2O4: Eu3+ crystals. Journal of Luminescence, 2019, 214, 116526.	1.5	1
136	Biosensors: Flexible, Graphene-Coated Biocomposite for Highly Sensitive, Real-Time Molecular Detection (Adv. Funct. Mater. 47/2016). Advanced Functional Materials, 2016, 26, 8796-8796.	7.8	0
137	Functionalized Natural Particles: Lightâ€Induced Surface Modification of Natural Plant Microparticles: Toward Colloidal Science and Cellular Adhesion Applications (Adv. Funct. Mater. 18/2018). Advanced Functional Materials, 2018, 28, 1870120.	7.8	0
138	Enhanced red emission in Yb3+/Ho3+/Cr3+ tridoped K2ErF5 microcrystal. Journal of Luminescence, 2020, 225, 117366.	1.5	0
139	Infrared Imaging Sensors: An Integrated Flexible Allâ€Nanowire Infrared Sensing System with Record Photosensitivity (Adv. Mater. 16/2020). Advanced Materials, 2020, 32, 2070126.	11.1	0